

Birck Nanotechnology Center

Other Nanotechnology Publications

Purdue Libraries

Year 2006

Atomistic simulations of long-range
strain and spatial asymmetry molecular
states of seven quantum dots

Marek Korkusinski*

Gerhard Klimeck†

*Purdue University - Main Campus,

†Purdue University - Main Campus, gekco@ecn.purdue.edu

This paper is posted at Purdue e-Pubs.

<http://docs.lib.purdue.edu/nanodocs/110>

Atomistic simulations of long-range strain and spatial asymmetry molecular states of seven quantum dots

Marek Korkusinski¹, Gerhard Klimeck^{1,2}

¹Network for Computational Nanotechnology, Purdue Univ., W. Lafayette IN 47907

²Jet Propulsion Laboratory, California Institute of Technology, Pasadena CA 91109

Corresponding author: Gerhard Klimeck, gekco@purdue.edu

Abstract. Coherent coupling and formation of molecular orbitals in vertically coupled quantum-dot molecules is studied for a seven-dot InAs/GaAs system. The electron states are computed using a nanoelectronic modelling tool NEMO-3D. The tool optimizes atomic positions in the sample with up to 64 million atoms in the frame of the atomistic VFF model. The resulting optimal interatomic distances are then used to formulate the 20-band sp³d⁵s* tight-binding Hamiltonian defined on a subdomain large enough to guarantee a correct treatment of confined orbitals. It is found that in the absence of strain (VFF optimization turned off), a clear and highly symmetric miniband structure of the seven-dot orbitals is formed. It maintains a high degree of symmetry even if the dots are taken to be realistically non-identical, where the dot size increases in the growth direction. However, the inclusion of strain breaks this symmetry completely. The simulations demonstrate the important interplay of strain engineering and size engineering in the design of quantum dot stacks.

1. Introduction

InAs/GaAs quantum dots (QDs) are semiconductor nanostructures producing a three-dimensional confinement both for electrons and holes [1]. The self-assembly of QDs is driven by strain, appearing as a result of the mismatch between lattice constants of constituent materials [1], and thus usually requires no lithography or etching. This makes QDs good candidates for optically active media of quantum-optical devices, such as detectors of infrared radiation [2], optical memories [1], and single photon sources [3]. Arrays of quantum-mechanically coupled QDs can also be used as optically active regions in high-efficiency, room-temperature lasers [4]. Of interest is therefore quantum-dot state engineering aimed at improving the electronic and optical properties of these systems.

This paper focuses on two possible methods of influencing the electronic properties of the systems. One of them involves strain, which strongly modifies the energy diagram of the system [5]. Due to its very long-range character, strain can be engineered by applying different boundary conditions to the sample. The second handle on the QD properties involves creating QD molecules – two or more dots aligned to allow quantum-mechanical coupling between them. Such multi-dot molecules are usually vertically self-aligned due to a strong directionality of the strain field [6]. Since even a small mismatch of energy levels in neighbouring dots can lead to qualitative changes in the device characteristics, simulations must treat the fundamental quantum character of charge carriers and the classical, long-distance strain effects on equal footing. The Nanoelectronic Modelling tool NEMO-3D [7] meets these requirements by modelling the strain and electronic structure of extended nanosystems (on the length scale of tens of nanometres, containing tens of millions of atoms) fully on the atomistic level.

2. The system

Two QD structures are considered. First, a single dome-shaped QD with diameter and height respectively of 18.09 nm and 1.7 nm, positioned on a 0.6-nm-thick wetting layer (figure 1(a)) is studied as a strain dependence benchmark for the NEMO-3D model. Second, electron states of a vertically coupled seven-disk molecule (figure 1(b)) are computed with and without strain, and, for each condition, assuming identical and nonidentical QDs. In each case, the computational strain domain, denoted in figure 1(a) by lateral size d and vertical size h , is taken to be much larger than the electronic structure domain. This is appropriate because in the electronic calculation only the confined states, decaying exponentially in the barrier, are targeted.

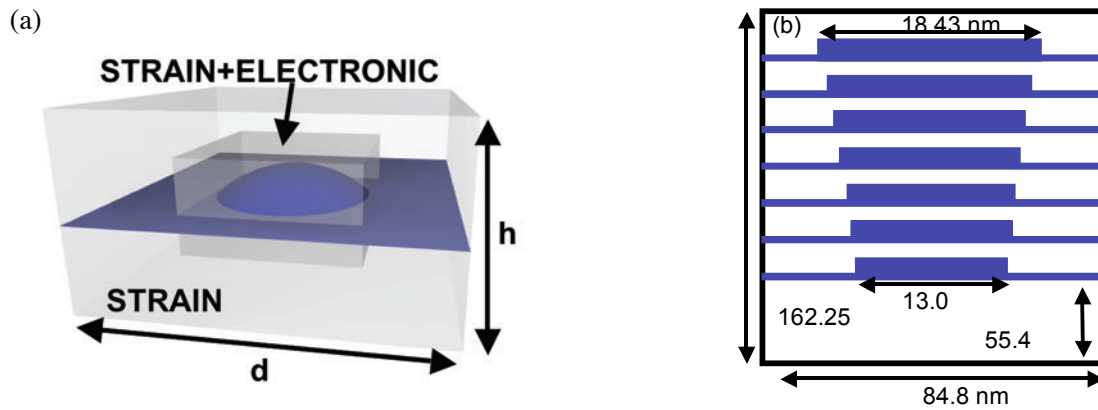


Fig. 1. (a) Schematic view of the single QD, with two simulation domains: central for electronic structure, and larger for strain calculations. (b) Cross-sectional view of the seven-dot molecule.

3. NEMO-3D

NEMO-3D is an atomistic simulation tool designed to provide *quantitative* predictions of the electronic structure of nanodevices [7]. The computation consists of two major steps. First, the strain distribution in the device is found by computing the positions of atoms yielding the minimal total elastic energy. Contributions to that energy from each distorted atomic bond are obtained in the frame of the VFF method with Keating potentials, and the minimization procedure employs the conjugate gradient technique. In the second step, an atomistic tight-binding Hamiltonian is used to find the electron and hole energy levels and wave functions of the system. This Hamiltonian is created in the basis of 20 orbitals per atom (spin-degenerate s , p , d , and s^*). Interactions between the orbitals within each atom and between the nearest neighbors are empirical fitting parameters, chosen so that the model reproduces the experimentally measured band structure of bulk semiconductors. Further, the tight-binding parameters are functions of interatomic bond length and angle distortions due to strain. The resulting Hamiltonian matrix is sparse; targeted eigenvalues and eigenvectors are found using the Lanczos algorithm.

Proper treatment of strain requires computational domains of tens of millions atoms. The electronic domains are usually smaller (up to 20 million atoms), but the $sp^3d^5s^*$ basis set results in Hamiltonian matrices of order of 20 times that number. Therefore, parallelization of NEMO-3D is a key consideration. The core computational engine of NEMO-3D was written in C with MPI used for message passing, which ensures its portability across major parallel computing platforms.

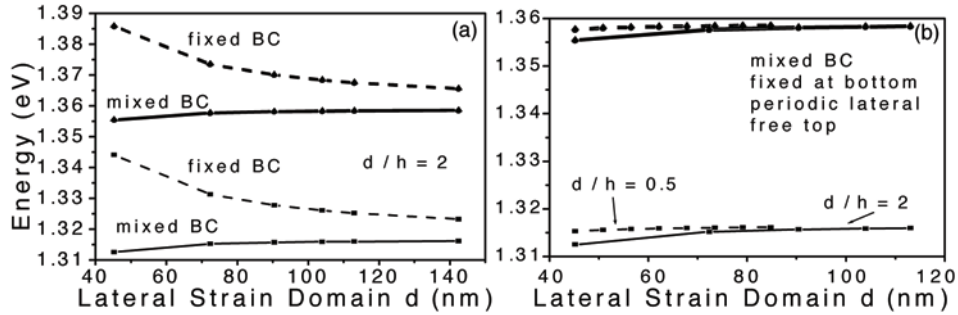


Fig. 2. Effect of long-range strain on the electronic ground state and first excited state. The lateral domain size is designated as “ d ” and the height of the strain domain as “ h ” as depicted in Fig. 1a. (a) comparison of the fixed BC (all edges of the domain fixed to GaAs lattice constant) and the mixed BC (fixed bottom, periodic lateral, free top). The free top BC allows the strain to relax in a significantly smaller lateral direction. (b) comparison of importance of lateral and horizontal strain extensions. Strain is predominantly vertically distributed as seen by smaller strain dependence on d for $d/h=0.5$.

The strain embedded in the quantum dot system has a significant effect on the electronic eigen energies of the system. The extent of the strain in the model structure depicted in Fig. 1a. is explored in Fig. 2. The fixed strain boundary condition (BC) corresponds to a deeply buried dot, where all bond lengths and positions are fixed to a GaAs bulk system at the edge of the simulation domain. Fig 2a indicates that under those conditions the strain reaches over 120nm in the lateral direction “ d ”. If the QD is not buried so deeply a mixed BC might be more appropriate: a fixed GaAs BC at the bottom, a periodic BC in the lateral directions and a free BC at the top. The strain relaxes over a significantly smaller lateral range. Fig 2b compared the importance of the lateral (d) vs. vertical (h) strain domain size. The solid line from Fig 2a is repeated in Fig 2b where $d/h=2$. For a strain domain that is larger in the vertical direction than the horizontal direction the lateral strain relaxes at a significantly shorter lateral distance. This indicates the strong vertical strain distribution and is one of the reasons for a preferred vertical quantum dot growth. The mixed BCs are employed in the remainder of this work.

4. Seven-dot molecule

NEMO-3D is applied to study several lowest electronic orbitals of a seven-disk molecule, whose schematic cross-section is shown in figure 1(b). Throughout this study the height of the disks is taken to be 2.83 nm above the wetting layer, and the distance between neighboring disks is 3.96 nm. As for the diameter of disks, two cases are considered: first, where all of them are identical and equal to 13 nm, and the second, where the diameter of the bottom disk is 13 nm, but it is gradually increased for the higher disks, reaching 18.43 nm for the top one. In both cases the strain domain is taken to contain 44.7 million atoms, and mixed BCs are applied to its walls. The electronic structure, on the other hand, is computed within the subdomain composed of 6.1 million atoms with fixed BCs.

The analysis starts with the system of identical dots. Figure 3(a) shows the vertical cross-section of the seven lowest electronic charge densities computed without strain, i.e., with the VFF optimization turned off. The high symmetry of the system leads to formation of highly regular molecular orbitals forming a miniband. All seven orbitals are of s -type in the XY plane, while along the vertical direction they exhibit an increasing number of nodes. The three top panels of figure 3(a) differ from the three bottom ones by symmetry: while the states E1-E3 are symmetric, the states E5-E7 are antisymmetric. Inclusion of strain under mixed BCs frustrates the symmetry of the system and leads to a renormalization of charge densities in favor of the lower part of the structure (figure 3(b)). Note, however, that the miniband symmetry appears to be restored in the orbitals E4-E7: they differ only slightly from their unstrained counterparts.

A radically different picture is seen for the molecule composed of nonidentical dots. In the unstrained case (figure 3(c)) the miniband symmetry is not present. Instead, the ground-state density is

biased in favor of the largest dot. It shifts towards smaller dots only for the higher-lying states. This tendency is counteracted by the strain, which favors the bottom dot (the smallest one, see figure 3(d)). As a result, the states E7 and E8 are somewhat similar to their counterparts seen in figure 3(b). Note, however, that the nonuniformity of the QD diameters leads to the appearance of a p-type state (E6) within the s-type miniband, in contrast to the previous three cases, where all the p orbitals lie well above the s-type miniband.

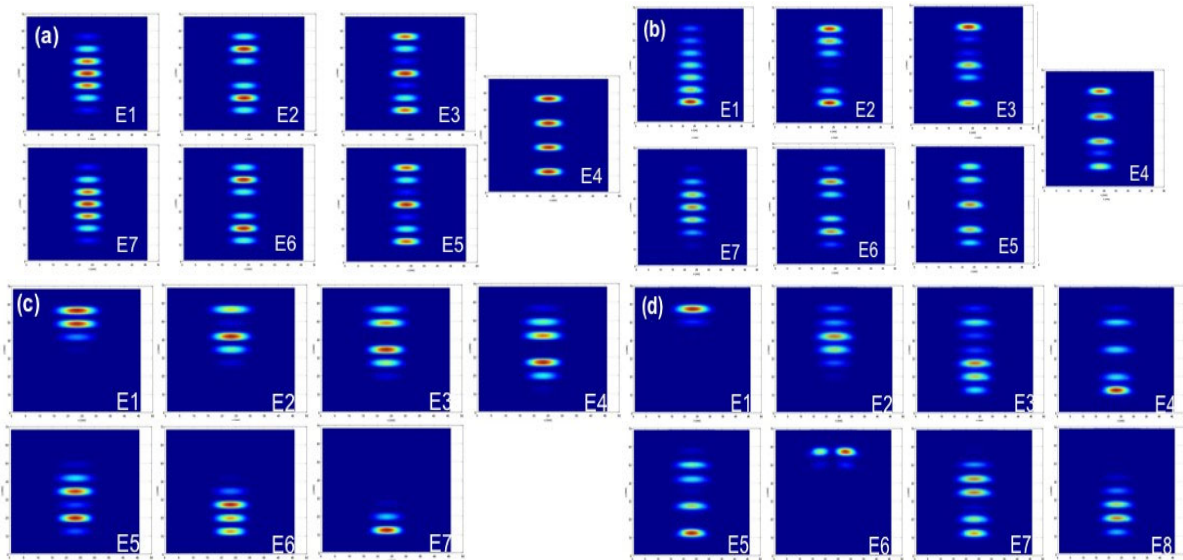


Fig. 3. Charge densities corresponding to the first few electronic states in the four cases: identical dots, without (a) and with strain (b), nonidentical dots without (c) and with strain (d).

5. Conclusions

The molecular states in various approximations of a 7 quantum dot molecule are computed. Strain induces an asymmetry which favors the ground state to be in the bottom dot while structural asymmetries favor the ground state at the top dot. Only detailed calculations of strain and electronic structure in realistically extended systems can deliver the required analytical tool to deliver quantitative device modeling needed for optical detector or laser design. NEMO 3-D does provide that capability and will be further used in the exploration of the QD design space.

6. Acknowledgements

Funding at Purdue was provided by NSF under Grant No. EEC-0228390 and by the Indiana 21st Century Fund. The work described in this publication was carried out in part at the Jet Propulsion Laboratory, California Institute of Technology under a contract with the National Aeronautics and Space Administration. At JPL funding was provided under grants from ONR, ARDA, and JPL.

References

- [1] For reviews and references, see “Single Quantum Dots: Fundamentals, Applications and New Concepts”, Michler, P, Ed., Springer, Berlin, 2003.
- [2] Aslan, B, Liu, H.C, Korkusinski, M, Cheng, S-J, Hawrylak, P, Appl. Phys. Lett., 82, 630, 2003
- [3] Michler, P, et al, Science, 290, 2282, 2000; Moreau, E, et al, Phys. Rev. Lett., 87, 183601, 2001.
- [4] Arakawa, Y, Sasaki, H, Appl. Phys. Lett., 40, 939, 1982; Fafard, S, et al, Science, 22, 1350, 1996; Maximov, M.V, et al., J. Appl. Phys., 83, 5561, 1998.
- [5] For a review and references see, e.g., Tadic, M, et al., J. Appl. Phys. 92, 5819, 2002.
- [6] Wasilewski, Z.R, Fafard, S, and McCaffrey, J.P, J. Cryst. Growth, 201, 1131, 1999.
- [7] Klimeck, G, et al, Computer Modeling in Engineering and Science, 3, 601, 2002; Oyafuso, F, et al, Journal of Computational Electronics, 1, 317, 2002.